

The limits of dynamical modelling

Eugene Vasiliev

University of Surrey

Galaxy Dynamics conference; Sexten, 7 July 2026



Giacomo Balla – Dynamism of a dog on a leash

Equilibrium models in stellar dynamics

Distribution function of stars $f(\mathbf{x}, \mathbf{v}, t)$ satisfies [sometimes] the collisionless Boltzmann equation:

$$\frac{\partial f(\mathbf{x}, \mathbf{v}, t)}{\partial t} + \frac{\partial f(\mathbf{x}, \mathbf{v}, t)}{\partial \mathbf{x}} \mathbf{v} - \frac{\partial f(\mathbf{x}, \mathbf{v}, t)}{\partial \mathbf{v}} \frac{\partial \Phi(\mathbf{x}, t)}{\partial \mathbf{x}} = 0.$$

observational data



potential \Leftrightarrow mass distribution



Equilibrium models in stellar dynamics

Distribution function of stars $f(\mathbf{x}, \mathbf{v}, t)$ satisfies [sometimes] the collisionless Boltzmann equation:

$$\frac{\partial f(\mathbf{x}, \mathbf{v}, t)}{\partial t} + \frac{\partial f(\mathbf{x}, \mathbf{v}, t)}{\partial \mathbf{x}} \mathbf{v} - \frac{\partial f(\mathbf{x}, \mathbf{v}, t)}{\partial \mathbf{v}} \frac{\partial \Phi(\mathbf{x}, t)}{\partial \mathbf{x}} = 0.$$

potential \Leftrightarrow mass distribution

observational data

not measured directly on human timescales

In order to infer anything about the potential from a time-dependent DF, need to make further assumptions about the initial state of the system, e.g., that the stars belong to a single stream or were perturbed from an equilibrium configuration in a specific way, etc.

Equilibrium models in stellar dynamics

Distribution function of stars $f(\mathbf{x}, \mathbf{v}, t)$ satisfies [sometimes] the collisionless Boltzmann equation:

$$\frac{\partial f(\mathbf{x}, \mathbf{v})}{\partial \mathbf{x}} \cdot \mathbf{v} - \frac{\partial f(\mathbf{x}, \mathbf{v})}{\partial \mathbf{v}} \cdot \frac{\partial \Phi(\mathbf{x})}{\partial \mathbf{x}} = 0.$$

Steady-state assumption \implies Jeans theorem:

$$f(\mathbf{x}, \mathbf{v}) = f(\mathcal{I}(\mathbf{x}, \mathbf{v}; \Phi))$$

3D - 6D
(observed)

integrals of motion ($\leq 3D?$), e.g., $\mathcal{I} = \{E, L, \dots\}$

3D function
(want to infer)

Equilibrium models in stellar dynamics

Distribution function of stars $f(\mathbf{x}, \mathbf{v}, t)$ satisfies [sometimes] the collisionless Boltzmann equation:

$$\frac{\partial f(\mathbf{x}, \mathbf{v})}{\partial \mathbf{x}} \cdot \mathbf{v} - \frac{\partial f(\mathbf{x}, \mathbf{v})}{\partial \mathbf{v}} \cdot \frac{\partial \Phi(\mathbf{x})}{\partial \mathbf{x}} = 0.$$

Steady-state assumption \implies Jeans theorem:

$$f(\mathbf{x}, \mathbf{v}) = f(\mathcal{I}(\mathbf{x}, \mathbf{v}; \Phi))$$

3D - 6D
(observed)

integrals of motion ($\leq 3D?$), e.g., $\mathcal{I} = \{E, L, \dots\}$

3D function
(want to infer)

When observations provide more than 3 phase-space coordinates, the potential is overconstrained! (can detect non-stationarity, but not measure it)

Self-consistent models in stellar dynamics

$$\iiint f(\mathcal{I}(\mathbf{x}, \mathbf{v}; \Phi)) d^3\mathbf{v} = \rho(\mathbf{x}) = \frac{1}{4\pi G} \nabla^2 \Phi(\mathbf{x}).$$

0th moment of the DF Poisson eqn

Ways to solve this integro-differential equations:

Self-consistent models in stellar dynamics

$$\iiint f(\mathcal{I}(\mathbf{x}, \mathbf{v}; \Phi)) d^3\mathbf{v} = \rho(\mathbf{x}) = \frac{1}{4\pi G} \nabla^2 \Phi(\mathbf{x}).$$

0th moment of the DF Poisson eqn

Ways to solve this integro-differential equations:

1. from ρ (and Φ , though they don't have to be related through the Poisson eqn) to f :
 - ▶ spherical systems (1d ρ, Φ): Eddington inversion (1d $f(E)$)
or its anisotropic generalisations $f(E, L)$
[Ossipkov 1979; Merritt 1985; Cuddeford 1991; Gerhard 1991; Wojtak+ 2008, ...]
 - ▶ axisymmetric (2d ρ, Φ): contour integral method $\Rightarrow f(E, L_z)$ [Hunter & Qian 1993],
but more general 3-integral DFs are possible [e.g. Dehnen & Gerhard 1993, Evans+ 1997]
 - ▶ triaxial (3d ρ, Φ): no general approach to derive 3d $f(\mathcal{I})$, but Schwarzschild
and M2M methods do it “numerically”

Self-consistent models in stellar dynamics

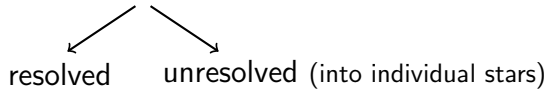
$$\iiint f(\mathcal{I}(\mathbf{x}, \mathbf{v}; \Phi)) d^3\mathbf{v} = \rho(\mathbf{x}) = \frac{1}{4\pi G} \nabla^2 \Phi(\mathbf{x}).$$

0th moment of the DF Poisson eqn

Ways to solve this integro-differential equations:

1. from ρ (and Φ , though they don't have to be related through the Poisson eqn) to f :
 - ▶ spherical systems (1d ρ, Φ): Eddington inversion (1d $f(E)$)
or its anisotropic generalisations $f(E, L)$
[Ossipkov 1979; Merritt 1985; Cuddeford 1991; Gerhard 1991; Wojtak+ 2008, ...]
 - ▶ axisymmetric (2d ρ, Φ): contour integral method $\Rightarrow f(E, L_z)$ [Hunter & Qian 1993],
but more general 3-integral DFs are possible [e.g. Dehnen & Gerhard 1993, Evans+ 1997]
 - ▶ triaxial (3d ρ, Φ): no general approach to derive 3d $f(\mathcal{I})$, but Schwarzschild
and M2M methods do it "numerically"
2. from f to ρ (and then Φ through Poisson eqn):
 - ▶ spherical systems: a few models defined by DFs (polytropes, King models, etc.)
 - ▶ more generally: iterative method [Kuijken & Dubinski 1995; Binney 2014]

Observational data



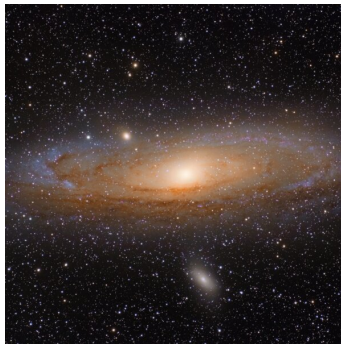
X, Y sky-plane position	+	+	(surface brightness profile)
Z distance	±	-	
$\mu_{X,Y}$ proper motions	±	-	
V_{los} line-of-sight velocity	±	+	(LoS velocity distribution).

Milky Way and LG galaxies

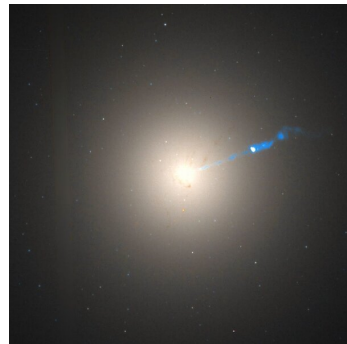
Galaxies outside the Local Group



Sculptor dSph [credit: Subaru]



Andromeda [Wikipedia / B.Wesner]



M 87 [HST]

Fitting models to observations

resolved data

DF-based methods:

$$\mathcal{P}(\text{model} \mid \text{data}) \propto \prod_{i=1}^{N_{\text{stars}}} f(\mathbf{x}_i, \mathbf{v}_i; \boldsymbol{\alpha}) = \prod_{i=1}^{N_{\text{stars}}} f\left(\mathcal{I}(\mathbf{x}_i, \mathbf{v}_i; \Phi(\mathbf{x}; \boldsymbol{\beta})); \boldsymbol{\alpha}\right),$$

where $\boldsymbol{\alpha}$, $\boldsymbol{\beta}$ are the parameters of the DF and the potential, respectively, which are optimised during model fitting;

in the self-consistent case, Φ is determined by the DF, so $\boldsymbol{\beta}$ are unused.

Fitting models to observations

resolved data

DF-based methods:

$$\mathcal{P}(\text{model} \mid \text{data}) \propto \prod_{i=1}^{N_{\text{stars}}} f(\mathbf{x}_i, \mathbf{v}_i; \boldsymbol{\alpha}) = \prod_{i=1}^{N_{\text{stars}}} f\left(\mathcal{I}(\mathbf{x}_i, \mathbf{v}_i; \Phi(\mathbf{x}; \boldsymbol{\beta})); \boldsymbol{\alpha}\right),$$

where $\boldsymbol{\alpha}$, $\boldsymbol{\beta}$ are the parameters of the DF and the potential, respectively, which are optimised during model fitting;

in the self-consistent case, Φ is determined by the DF, so $\boldsymbol{\beta}$ are unused.

Jeans models:

fit for spatially binned moments $(\bar{\mathbf{v}}, \sigma)$,

or assume a Gaussian DF $f = \rho(\mathbf{x}) \mathcal{N}(\mathbf{v} \mid \sigma(\mathbf{x}))$ and proceed as above (possibly a more complicated $f(\mathbf{v})$ when using higher-order Jeans eqns)

Fitting models to observations

resolved data

DF-based methods:

$$\mathcal{P}(\text{model} \mid \text{data}) \propto \prod_{i=1}^{N_{\text{stars}}} f(\mathbf{x}_i, \mathbf{v}_i; \boldsymbol{\alpha}) = \prod_{i=1}^{N_{\text{stars}}} f(\mathcal{I}(\mathbf{x}_i, \mathbf{v}_i; \Phi(\mathbf{x}; \boldsymbol{\beta})); \boldsymbol{\alpha}),$$

where $\boldsymbol{\alpha}$, $\boldsymbol{\beta}$ are the parameters of the DF and the potential, respectively, which are optimised during model fitting;

in the self-consistent case, Φ is determined by the DF, so $\boldsymbol{\beta}$ are unused.

Jeans models:

fit for spatially binned moments $(\bar{\mathbf{v}}, \sigma)$,

or assume a Gaussian DF $f = \rho(\mathbf{x}) \mathcal{N}(\mathbf{v} \mid \sigma(\mathbf{x}))$ and proceed as above (possibly a more complicated $f(\mathbf{v})$ when using higher-order Jeans eqns)

Orbit-based methods:

conceptually difficult... [e.g. Chaname+ 2008]

Fitting models to observations

resolved data

DF-based methods:

$$\mathcal{P}(\text{model} \mid \text{data}) \propto \prod_{i=1}^{N_{\text{stars}}} f(\mathbf{x}_i, \mathbf{v}_i; \boldsymbol{\alpha}) = \prod_{i=1}^{N_{\text{stars}}} f(\mathcal{I}(\mathbf{x}_i, \mathbf{v}_i; \Phi(\mathbf{x}; \boldsymbol{\beta})); \boldsymbol{\alpha}),$$

where $\boldsymbol{\alpha}$, $\boldsymbol{\beta}$ are the parameters of the DF and the potential, respectively, which are optimised during model fitting;

in the self-consistent case, Φ is determined by the DF, so $\boldsymbol{\beta}$ are unused.

Jeans models:

fit for spatially binned moments (\bar{v}, σ) ,

or assume a Gaussian DF $f = \rho(\mathbf{x}) \mathcal{N}(\mathbf{v} \mid \sigma(\mathbf{x}))$ and proceed as above (possibly a more complicated $f(\mathbf{v})$ when using higher-order Jeans eqns)

Orbit-based methods:

conceptually difficult... [e.g. Chaname+ 2008]

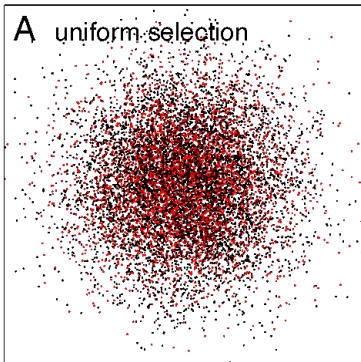
unresolved data

fit surface density $\Sigma(X, Y)$ and 3d LOSVD $f(X, Y, v_{\text{los}})$,

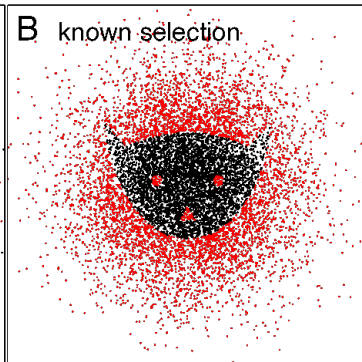
represented by velocity histograms or Gauss–Hermite moments

Episode 1: Fitting models to incomplete observations

Introduce the [spatial] selection function $S(\mathbf{x})$ – fraction of stars included in the kinematic sample



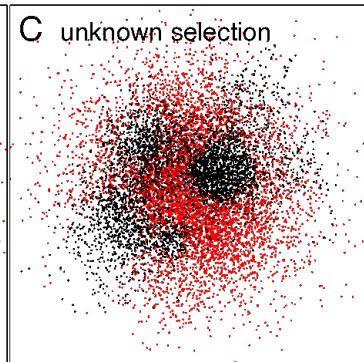
$$\ln \mathcal{L} = \sum_{i=1}^{N_{\text{stars}}} \ln f(\mathbf{x}_i, \mathbf{v}_i)$$



$$\ln \mathcal{L} = \sum_{i=1}^{N_{\text{stars}}} \ln \frac{f(\mathbf{x}_i, \mathbf{v}_i)}{\mathcal{N}},$$

$$\mathcal{N} \equiv \iiint d^3\mathbf{x} \iiint d^3\mathbf{v} f(\mathbf{x}, \mathbf{v}) S(\mathbf{x})$$

(normalization factor)



$$\ln \mathcal{L} = \sum_{i=1}^{N_{\text{stars}}} \ln f(\mathbf{v}_i | \mathbf{x}_i),$$

$$f(\mathbf{v} | \mathbf{x}) \equiv \frac{f(\mathbf{x}, \mathbf{v})}{\iiint d^3\mathbf{v} f(\mathbf{x}, \mathbf{v})} = \frac{f(\mathbf{x}, \mathbf{v})}{\rho(\mathbf{x})}$$

(conditional velocity distribution)

Episode 1: Fitting models to incomplete observations

Introduce the [spatial] selection function $S(\mathbf{x})$ – fraction of stars included in the kinematic sample

A uniform selection

B known selection

C unknown selection

Can one do dynamics
without knowing where
[all] the tracers are?

$$\ln \mathcal{L} = \sum_{i=1}^{N_{\text{stars}}} \ln f(\mathbf{x}_i, \mathbf{v}_i)$$

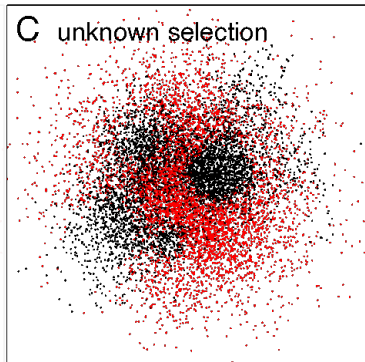
$$\ln \mathcal{L} = \sum_{i=1}^{N_{\text{stars}}} \ln \frac{f(\mathbf{x}_i, \mathbf{v}_i)}{\mathcal{N}},$$

$$\mathcal{N} \equiv \iiint d^3\mathbf{x} \iiint d^3\mathbf{v} f(\mathbf{x}, \mathbf{v}) S(\mathbf{x})$$

(normalization factor)

$$\ln \mathcal{L} = \sum_{i=1}^{N_{\text{stars}}} \ln f(\mathbf{v}_i | \mathbf{x}_i),$$
$$f(\mathbf{v} | \mathbf{x}) \equiv \frac{f(\mathbf{x}, \mathbf{v})}{\iiint d^3\mathbf{v} f(\mathbf{x}, \mathbf{v})} = \frac{f(\mathbf{x}, \mathbf{v})}{\rho(\mathbf{x})}$$

(conditional velocity distribution)



Toy example #1: one-dimensional vertical dynamics in a disc

Context: measure the gravitational potential $\Phi(z)$ or equivalently the force $\frac{d\Phi}{dz}(z)$ from stellar tracers at different heights z ;
not assuming that the potential is created by stars only (non-self-consistent).

1st approach: vertical Jeans equation

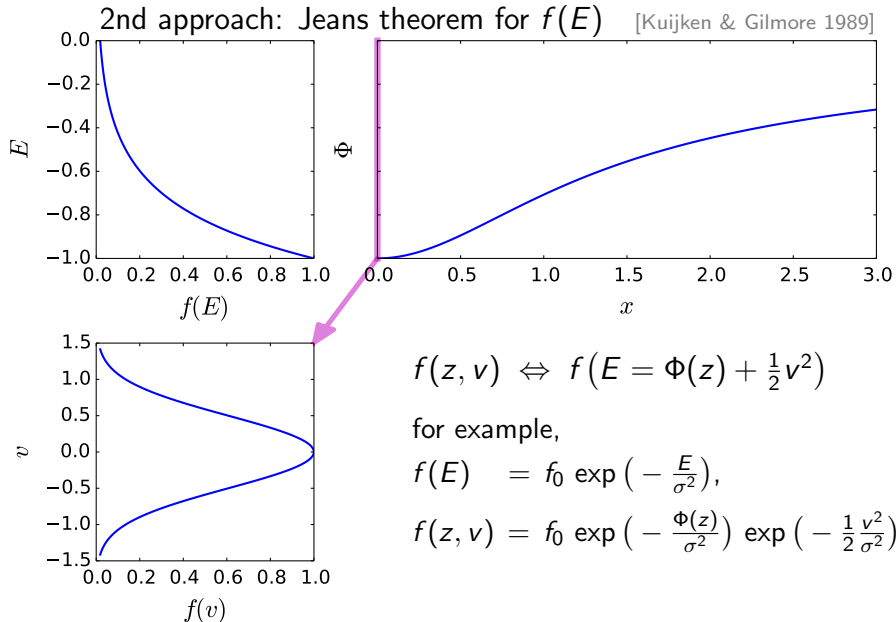
$$\frac{d(\rho \sigma^2)}{dz} + \rho \frac{d\Phi}{dz} = 0$$

$$\left(\frac{d \ln \rho}{dz} \right) + \frac{d\sigma^2}{dz} = \frac{d\Phi}{dz}$$

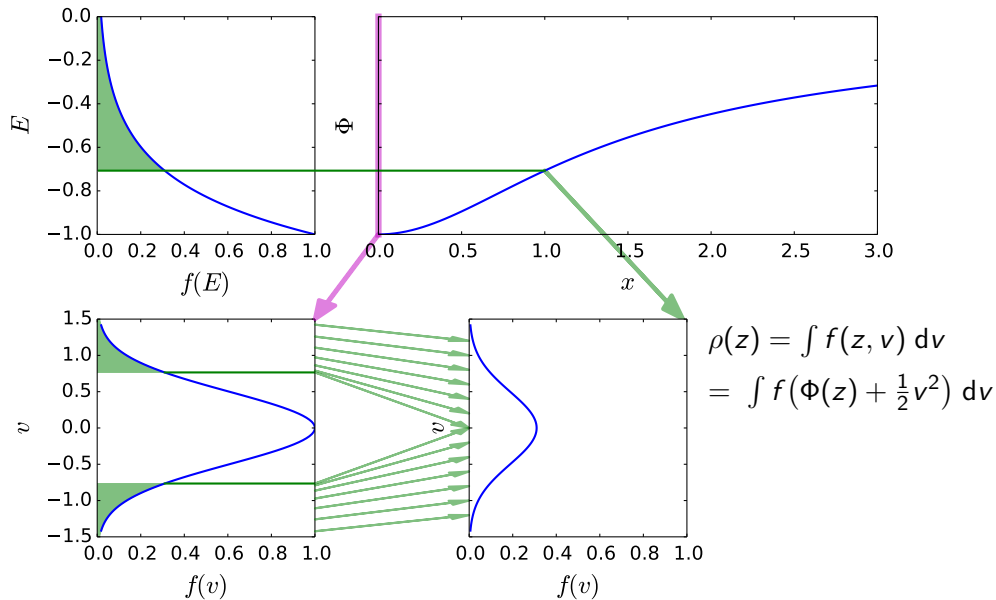
typically the dominant term

workflow: $\rho(z), \sigma(z) \Rightarrow \Phi(z)$.

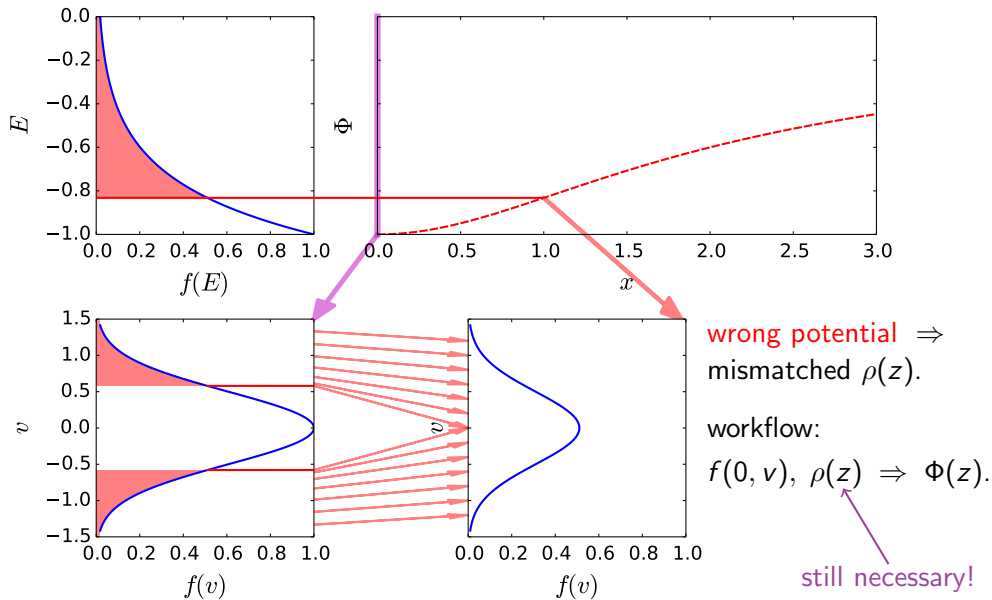
Toy example #1: one-dimensional vertical dynamics in a disc



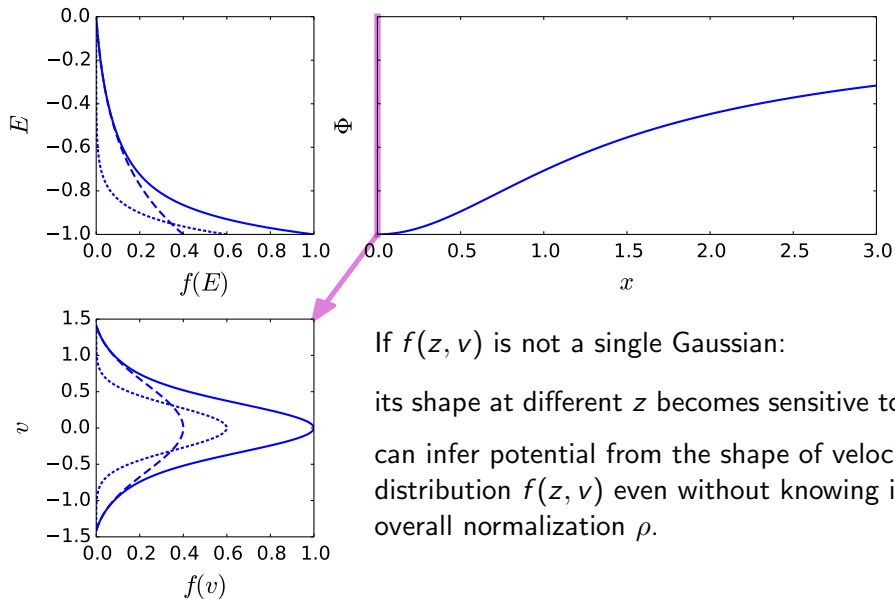
Toy example #1: one-dimensional vertical dynamics in a disc



Toy example #1: one-dimensional vertical dynamics in a disc



Toy example #1: one-dimensional vertical dynamics in a disc

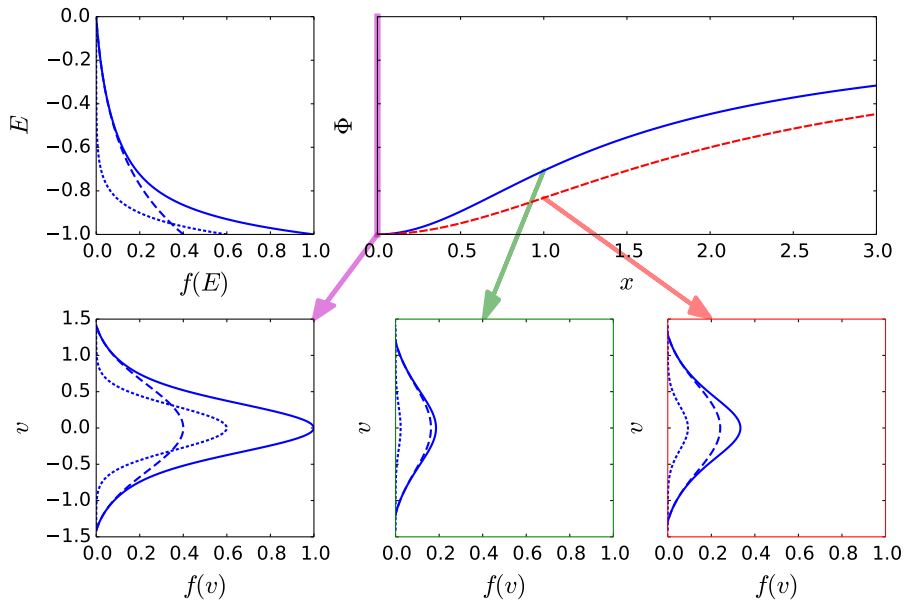


If $f(z, v)$ is not a single Gaussian:

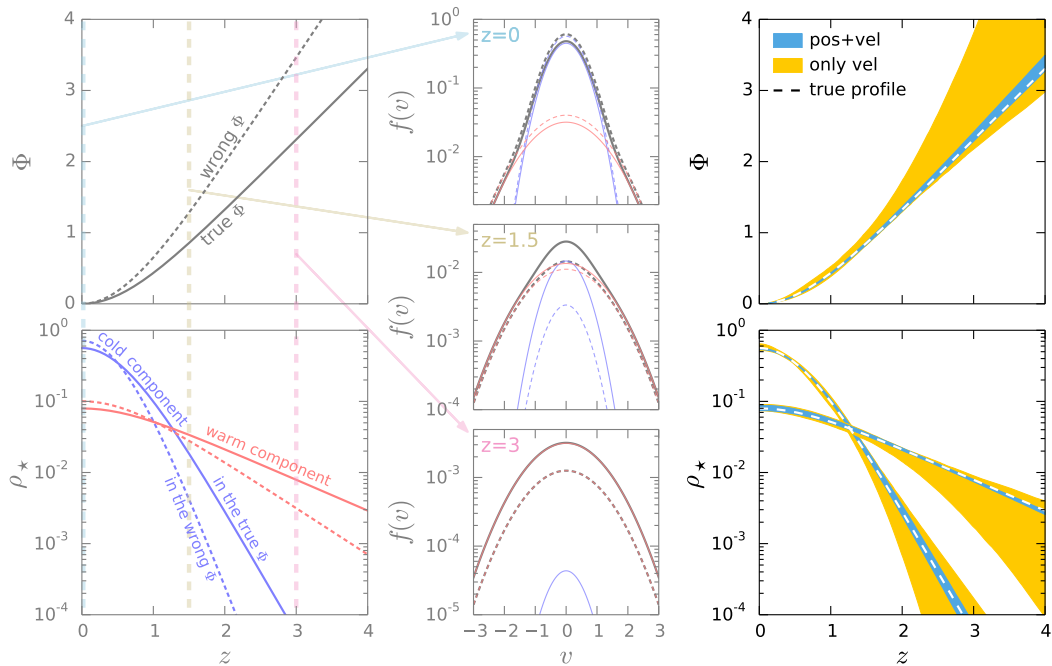
its shape at different z becomes sensitive to $\Phi \Rightarrow$

can infer potential from the shape of velocity distribution $f(z, v)$ even without knowing its overall normalization ρ .

Toy example #1: one-dimensional vertical dynamics in a disc



Toy example #1: one-dimensional vertical dynamics in a disc



Toy example #2: spherical galaxy

fitted parameters:

self-consistent

$$f(\mathcal{I}(\mathbf{x}, \mathbf{v}; \Phi); \alpha) \implies \rho(\mathbf{x})$$

$\Phi(\mathbf{x})$

α (DF)

The diagram for the self-consistent case shows the equation $f(\mathcal{I}(\mathbf{x}, \mathbf{v}; \Phi); \alpha) \implies \rho(\mathbf{x})$ at the top. Below it is the potential $\Phi(\mathbf{x})$. A red arrow points from $\Phi(\mathbf{x})$ to the Φ in the equation, and a pink arrow points from $\rho(\mathbf{x})$ to the Φ in the equation, indicating a mutual dependency.

non-self-consistent

$$f(\mathcal{I}(\mathbf{x}, \mathbf{v}; \Phi); \alpha) \implies \rho(\mathbf{x})$$
$$\Phi_{\text{ext}}(\mathbf{x}; \beta) \implies \rho_{\text{ext}}(\mathbf{x})$$

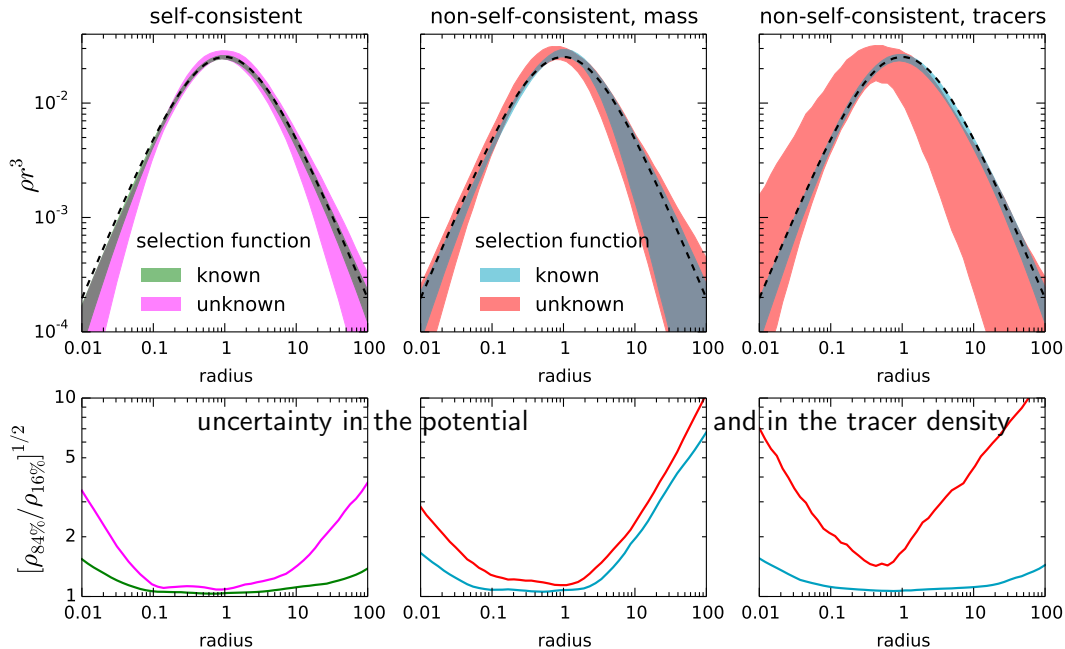
α (DF), β (potential)

The diagram for the non-self-consistent case shows two separate equations. The top equation is $f(\mathcal{I}(\mathbf{x}, \mathbf{v}; \Phi); \alpha) \implies \rho(\mathbf{x})$. Below it is $\Phi_{\text{ext}}(\mathbf{x}; \beta) \implies \rho_{\text{ext}}(\mathbf{x})$. A red arrow points from Φ_{ext} to the Φ in the top equation, indicating that the external potential is used in the main system's calculation.

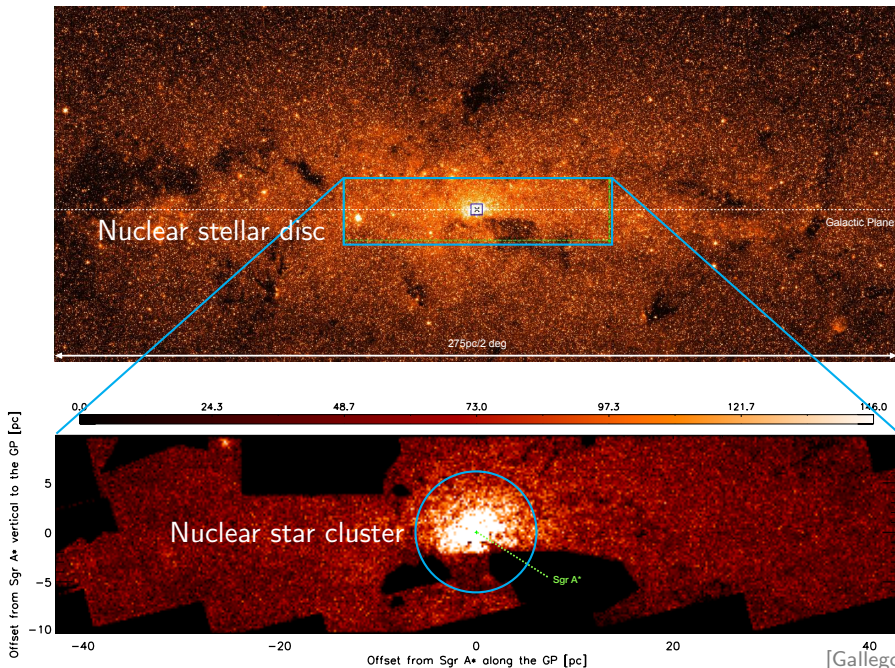
Toy example #2: spherical galaxy

	self-consistent	non-self-consistent
fitted parameters:	$f(\mathcal{I}(\mathbf{x}, \mathbf{v}; \Phi); \alpha) \implies \rho(\mathbf{x})$ $\alpha \text{ (DF)}$	$f(\mathcal{I}(\mathbf{x}, \mathbf{v}; \Phi); \alpha) \implies \rho(\mathbf{x})$ $\Phi_{\text{ext}}(\mathbf{x}; \beta) \implies \rho_{\text{ext}}(\mathbf{x})$ $\alpha \text{ (DF)}, \beta \text{ (potential)}$
known SF $\mathcal{L}_i = f(\mathbf{x}_i, \mathbf{v}_i)$		
unknown SF $\mathcal{L}_i = \frac{f(\mathbf{x}_i, \mathbf{v}_i)}{\rho(\mathbf{x})}$		

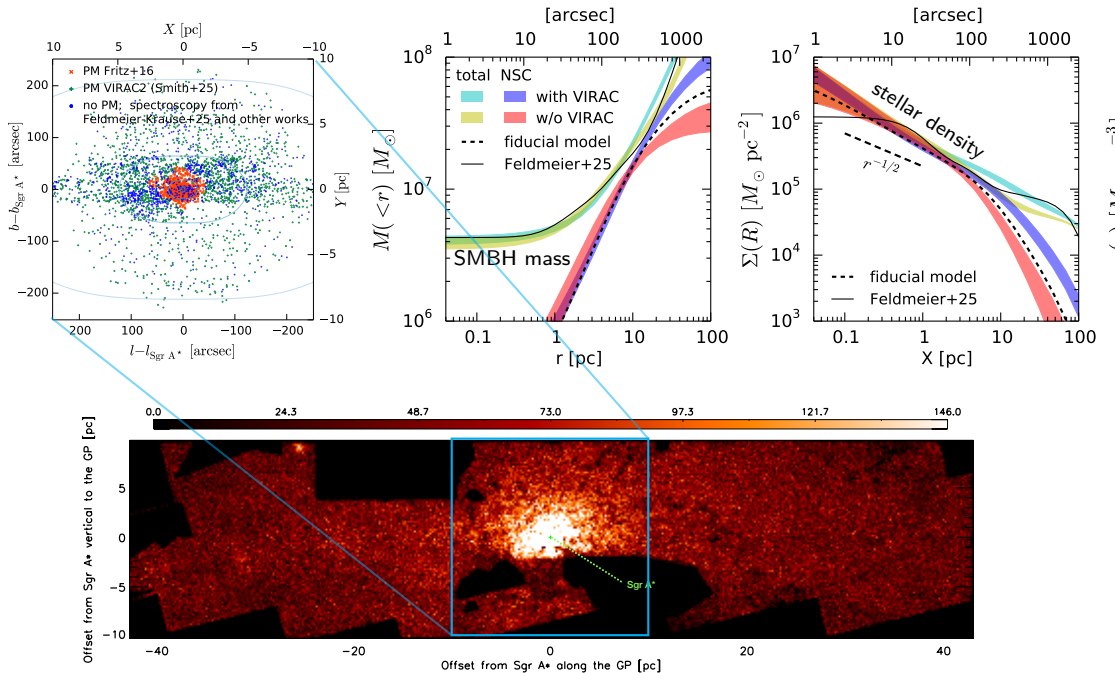
Toy example #2: spherical galaxy



Real application: Milky Way nuclear star cluster



Real application: Milky Way nuclear star cluster [Vasiliev+ 2026]



Episode 2: measuring the shape of the potential [Gherghinescu+ 2026]

Context:

constrain the shape of the dark matter haloes in external galaxies using discrete-kinematic tracers:

- ▶ stars in dSph galaxies around MW, or
- ▶ star clusters and PNe in galaxies like M31.

Ingredients:

axisymmetric dark halo potential Φ_{ext} created by an oblate density profile $\rho(\sqrt{R^2 + (z/q)^2})$, $q \leq 1$ (e.g. a generalised NFW) at inclination i ;

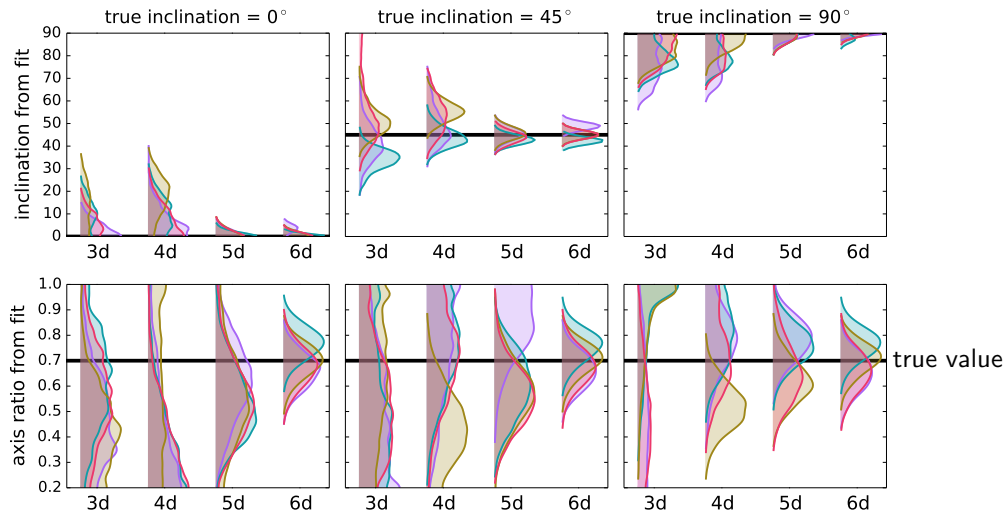
DF $f(\mathcal{I})$ for the tracer population; not self-consistent.

$N_{\star} \sim \mathcal{O}(10^3)$ tracers with incomplete phase-space information:
sky coordinates X, Y and

- ▶ 3d: v_{LoS} only;
- ▶ 4d: sky-plane velocities v_X, v_Y ;
- ▶ 5d: all three velocity components, but no distance;
- ▶ 6d: everything known.

Constraints on the potential from DF fits

- ✓ sphericalised density profile and inclination are well recovered
- ✗ halo shape q is **not** tightly constrained with 3d, 4d or even 5d data
- ✗ large variation between different realisations of mock data



Constraints on the potential from Schwarzschild models

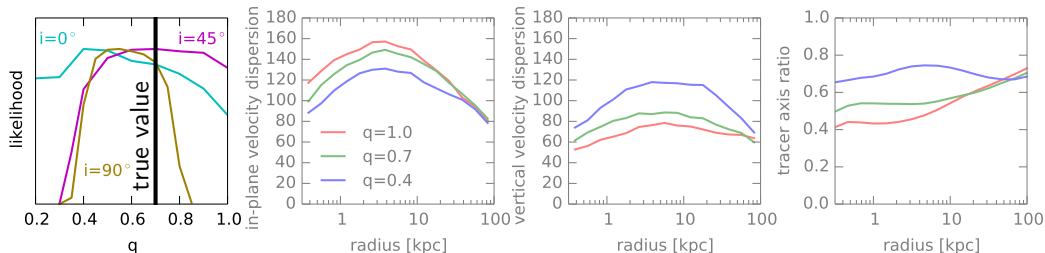
Could it be a limitation of the DF-based method?

another test: Schwarzschild models of integrated-light kinematics

(S/N equivalent to $\mathcal{O}(10^6)$ discrete tracers,

100+ bins with 8 Gauss-Hermite moments,

spatial coverage up to 100 kpc $\gtrsim 10 R_{\text{eff}}$).



Results: no constraints on the axis ratio q for face-on orientation ($i = 0^\circ$), and still quite weak constraints for edge-on ($i = 90^\circ$).

Enough internal freedom in the model to rearrange radial and vertical velocity distributions to keep the same line-of-sight kinematics.

Another test: constraints on shape and inclination

Setup:

Oblate Perfect Ellipsoid potential with axis ratio q , self-consistent (no DM halo);
kinematic data (6 GH moments) within region containing 90% of total luminosity;
different combinations of q and i giving the same projected axis ratio $\simeq 0.8$;
two free parameters – i and mass-to-light ratio M/L .

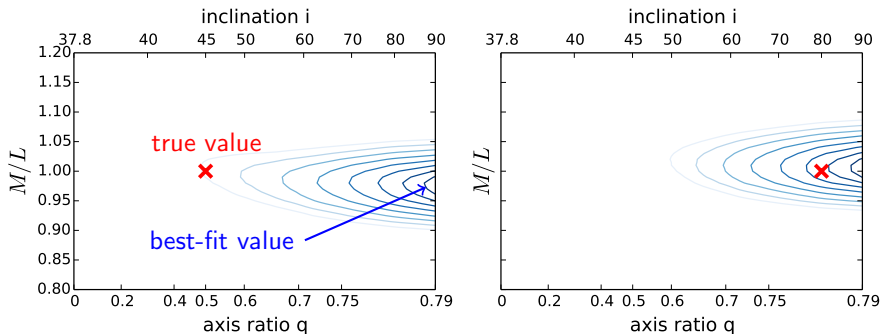
Another test: constraints on shape and inclination

Setup:

Oblate Perfect Ellipsoid potential with axis ratio q , self-consistent (no DM halo); kinematic data (6 GH moments) within region containing 90% of total luminosity; different combinations of q and i giving the same projected axis ratio $\simeq 0.8$; two free parameters – i and mass-to-light ratio M/L .

Result:

total disaster – regardless of true i , fits always prefer $i = 90^\circ$ [Thomas+ 2007]



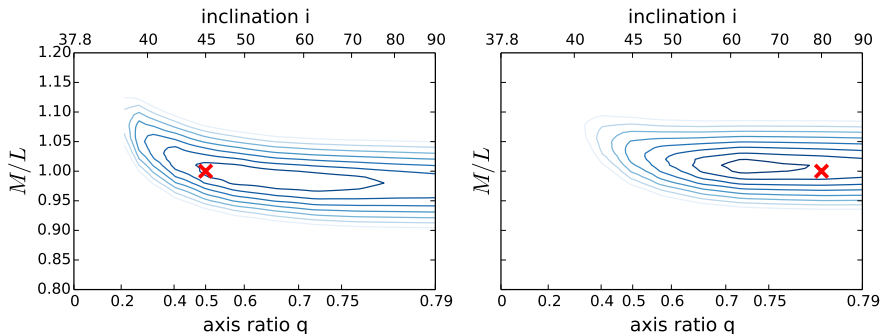
Another test: constraints on shape and inclination

Setup:

Oblate Perfect Ellipsoid potential with axis ratio q , self-consistent (no DM halo); kinematic data (6 GH moments) within region containing 90% of total luminosity; different combinations of q and i giving the same projected axis ratio $\simeq 0.8$; two free parameters – i and mass-to-light ratio M/L .
add the penalty for model flexibility to raw χ^2 values [Lipka & Thomas+ 2021].

Result:

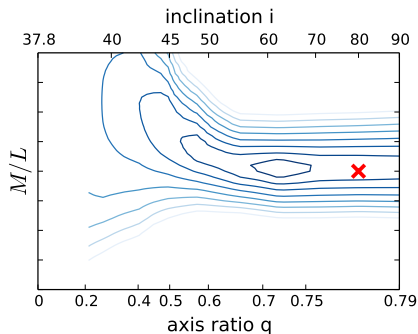
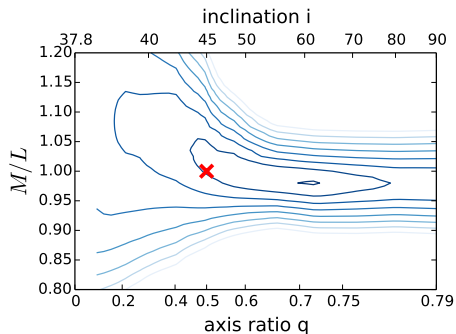
bias is gone, but constraints on i (and hence q) are pretty weak! [see also Krajnović+ 2005]



Another test: constraints on shape and inclination

Setup:

Oblate Perfect Ellipsoid potential with axis ratio q_{pot} , **non-self-consistent**: fit only the surface density profile and kinematics, but not 3d density constraints; q_{pot} and i are now decoupled, but even if we keep them linked as before, the constraints are even weaker.



Summary

- ▶ One can do meaningful dynamical modelling even without knowing the density profile of kinematic tracers \implies could be useful to sidestep complex selection functions or patchy extinction.
- ▶ The shape of an [axisymmetric] potential is difficult to constrain (though this does not impact the measurement of a sphericalized mass profile). Other studies [de Nicola+ 2022, Neureiter+ 2023; Veršič+ 2024] are more optimistic – need to understand the disagreement...

Summary

- ▶ One can do meaningful dynamical modelling even without knowing the density profile of kinematic tracers \implies could be useful to sidestep complex selection functions or patchy extinction.
- ▶ The shape of an [axisymmetric] potential is difficult to constrain (though this does not impact the measurement of a sphericalized mass profile). Other studies [de Nicola+ 2022, Neureiter+ 2023; Veršič+ 2024] are more optimistic – need to understand the disagreement...

